26291) and to the Matthey-Bishop Corp. for a generous loan of rhodium trichloride. K. H. Theopold acknowledges an Ephraim Weiss Scholarship (1980-1981) and a D. O. Sumek and S. M. Tasheira Scholarship (1981-1982) from the University of California, Berkeley. The X-ray structure analysis was performed by Dr. F. J. Hollander of the U. C. Berkeley X-ray diffraction facility (CHEXRAY). Funds for the analysis were provided by the above NSF grant; partial funding for the equipment in the facility was provided by NSF Grant CHE 79-07027.

Registry No. **1**, 77674-08-9; **1**-d_2, 84040-86-8; **2**, 84064-05-1; **2**-d_6, 84064-10-8; **3**, 84049-85-4; **4**, 84064-06-2; **4**-d_6, 84049-88-7; **5**, 84040-83-5; **5**-d_4, 84064-11-9; **6**, 79255-87-1; **7**, 84064-07-3; **8**, 84049-86-5; **9**, 84064-08-4; **9**-d_4, 84040-88-0; *cis*-**10**, 84040-84-6; *trans*-**10**, 84064-13-1; **11**, 84064-09-5; **12**, 84064-25-5; *trans*-**13**, 79390-72-0; *cis*-**13**, 77674-11-4; *trans*-**14**, 65138-22-9; *cis*-**14**, 84064-12-0; **15**, 69393-67-5; **16**, 77674-13-6; **18**, 84049-87-6; $Na[CpCo(CO)]_2$, 62602-00-0; CD_2I_2, 15729-58-5; $MeCpCo(CO)_2$, 12145-31-2; $NaCo(CO)_4$, 14878-28-5; $Na[MeCpCo(CO)]_2$, 84040-87-9; $CpRh(CO)_2$, 12192-97-1; $CpCo(CO)(C_2H_4)$, 77674-12-5; $[CpCo(CO)]_2$, 58496-39-2; diiodomethane, 75-11-6; 2,2-diiodopropane, 630-13-7; 1,1-diiodopropane, 10250-52-9; 3,3-diiodopropane, 66688-39-9; 2,2-diiodopentane, 66688-37-7; 1,1-diiodopentane, 66688-35-5; 1,1-diiodo-3,3-dimethylbutane, 84040-85-7; 2,2-diiodopropane-d_6, 79255-38-2; 2,2,4,4-tetradeuterio-3,3-diiodopentane, 79255-39-3.

Supplementary Material Available: A listing of observed and calculated structure factors (9 pages). Ordering information is given on any current masthead page.

Single Cubane-Type MFe_3S_4 Clusters (M = Mo, W): Synthesis and Properties of Oxidized and Reduced Forms and the Structure of $(Et_4N)_3[MoFe_3S_4(S\text{-}p\text{-}C_6H_4Cl)_4(3,6\text{-}(C_3H_5)_2C_6H_2O_2)]$

P. K. Mascharak, W. H. Armstrong, Y. Mizobe, and R. H. Holm*

Contribution from the Department of Chemistry, Harvard University, Cambridge, Massachusetts 02138. *Received May 3, 1982*

Abstract: Reaction of the solvated cubane-type clusters $[MFe_3S_4(SR)_3((C_3H_5)_2cat)(MeCN)]^{2-}$ (M = Mo, W; R = Et, p-C_6H_4Cl; $(C_3H_5)_2cat$ = 3,6-diallylcatecholate) with the ligands L = p-$ClC_6H_4S^-$, PhO^-, CN^- and PEt_3 affords the ligated clusters $[MFe_3S_4(SR)_3((C_3H_5)_2cat)L]^{2-,3-}$. Examples of each, except phosphine clusters, have been isolated as Et_4N^+ salts in 54-77% yields. $(Et_4N)_3[MoFe_3S_4(S\text{-}p\text{-}C_6H_4Cl)_4((C_3H_5)_2cat)]$ crystallizes in monoclinic space group $C2/c$ with a = 33.918 (8) Å, b = 16.674 (4) Å, c = 27.374 (5) Å, β = 95.98 (2)°, and Z = 8. On the basis of 5511 unique data ($F_o^2 > 2.5\sigma(F_o)^2$) the structure was refined to R = 6.6%. The structure provides the first definitive proof of a *single* MFe_3S_4 cubane-type cluster, which in this compound approaches C_s symmetry. Solvated clusters exhibit chemically reversible one-electron reduction reactions, and solutions of $[MFe_3S_4(S\text{-}p\text{-}C_6H_4Cl)_3((C_3H_5)cat)(MeCN)]^{3-}$ are readily prepared by reduction of solvated 2- clusters with sodium acenaphthylenide. The reduced clusters are paramagnetic (probable S = 2 ground state) and form 1:1 adducts with PEt_3 and CO. ^1H NMR spectra demonstrate that all oxidized and reduced ligated clusters have structures of effective C_s symmetry in solution. Other results relevant to the reactions of oxidized and reduced clusters and π donor properties of the latter are presented. The availability and spectroscopic characterization of reduced clusters, with substitutionally labile solvate molecules at the Mo atom site, provide an opportunity to examine reactions of nitrogenase substrates at that site.

Evolvement of the chemistry of MFe_3S_4 clusters (M = Mo, W) is detailed in recent reports from this laboratory,[1-6] in which we describe our interest in these species as the only examples of mixed-metal $M'_nM_{4-n}S_4$ cubane-type clusters and as preliminary models of the Mo atom coordination unit in nitrogenase. An important aspect of this research continues to be synthesis and physicochemical and reactivity characterization of *single* cubane species. These are not accessible from cluster assembly reactions which afford various types of bridged *double* cubanes[3,7-10] (e.g., $[M_2Fe_6S_8(\mu_3\text{-}SR)_3(SR)_6]^{3-}$) depending on conditions.

Our approach to the synthesis of single cubanes is outlined in Figure 1. Reaction 1, in which the Fe(III)-bridged double cubane $[M_2Fe_7S_8(SR)_{12}]^{3-}$[8,9] (**1**-M) is treated with a 3,6-disubstituted catechol ($R_{3,6}$ = $CH_2CH{=}CH_2$, *n*-Pr), results in bridge disruption and formation of the doubly bridged double cubane $[M_2Fe_6S_8(SR)_6(R_{3,6}\text{-}cat)_2]^{4-}$[1,5,11] (**2**-M). In coordinating solvents this species, in reaction 2, experiences bridge cleavage to form the solvated single cubane $[MFe_3S_4(SR)_3(R_{3,6}\text{-}cat)(solv)]^{2-}$[1,5] (**3**-M). This cluster undergoes the thiolate ligand substitution reaction 3,[5] and the solvent displacement reaction 4 with ligands $L^{0,1-}$ to afford single cubanes $[MFe_3S_4(SR)_3(R_{3,6}\text{-}cat)L]^{2-,3-}$.[4,5] The structures of two key intermediate clusters **2**-Mo (R = Et, Ph) have been established by X-ray diffraction.[1,5,12]

(1) Armstrong, W. H.; Holm, R. H. *J. Am. Chem. Soc.* **1981**, *103*, 6246.
(2) Palermo, R. E.; Power, P. P.; Holm, R. H. *Inorg. Chem.* **1982**, *21*, 173.
(3) Christou, G.; Mascharak, P. K.; Armstrong, W. H.; Papaefthymiou, G. C.; Frankel, R. B.; Holm, R. H. *J. Am. Chem. Soc.* **1982**, *104*, 2820.
(4) Armstrong, W. H.; Mascharak, P. K.; Holm, R. H. *Inorg. Chem.* **1982**, *21*, 1699.
(5) Armstrong, W. H.; Mascharak, P. K.; Holm, R. H. *J. Am. Chem. Soc.* **1982**, *104*, 4373.
(6) Holm, R. H. *Chem. Soc. Rev.* **1981**, *10*, 455.
(7) Wolff, T. E.; Berg, J. M.; Hodgson, K. O.; Frankel, R. B.; Holm, R. H. *J. Am. Chem. Soc.* **1979**, *101*, 4140.
(8) Wolff, T. E.; Berg, J. M.; Power, P. P.; Hodgson, K. O.; Holm, R. H. *Inorg. Chem.* **1980**, *19*, 430.
(9) Wolff, T. E.; Power, P. P.; Frankel, R. B.; Holm, R. H. *J. Am. Chem. Soc.* **1980**, 102, 4694.
(10) Christou, G.; Garner, C. D. *J. Chem. Soc., Dalton Trans.* **1980**, 2354.
(11) A different cluster product, $[MoFe_3S_4(SEt)_3Fe(cat)_3]^{3-}$, is obtained from the reaction of **1**-Mo (R = Et) with catechol itself: Wolff, T. E.; Berg, J. M.; Holm, R. H. *Inorg. Chem.* **1981**, *20*, 174.
(12) Armstrong, W. H. Ph.D. Thesis, Stanford University, 1982.

0002-7863/83/1505-0475$01.50/0

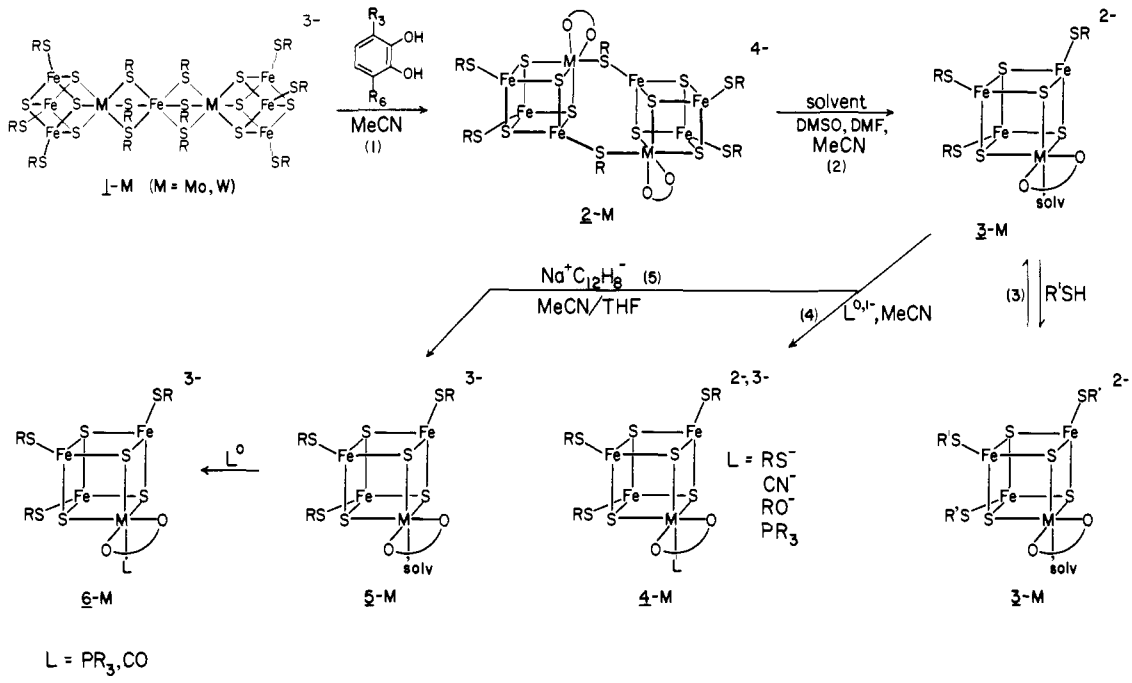

Figure 1. Schematic representation of the formation and reactions of the single-cubane clusters **3**-M, **4**-M, **5**-M, and **6**-M.

The clusters **3**-M are of particular interest in the problem of modeling the Mo atom site in nitrogenase. These species have a $S = {}^3/_2$ ground state,[1,5] as does the Fe–Mo–S cluster of the enzyme[13,14] and its cofactor[15] (FeMo-co), a labile Mo coordination site for binding of potential substrates, and a reduced form (**5**-M) which has been detected electrochemically.[5] Because crystallization of salts of **3**-M results in the isolation of compounds containing **2**-M in the solid state,[5] we have utilized reaction 4 to provide single cubanes isolable as such in the crystalline state.[4] Here we provide more extensive documentation of the occurrence of this reaction, including characterization of clusters **4**-M, and a detailed structure of one of them, with L = S-*p*-C_6H_4Cl. Also included are qualitative comparative reactivity studies of oxidized (**3**-M) and reduced (**5**-M) solvated clusters with selected ligands.

Experimental Section

With reference to Figure 1 the designations used hereafter for the various cluster species are the following: **2**-M-R, **3**-M-R-solv, **4**-M-R-L, **5**-M-R-solv, **6**-M-R-L. When R = *p*-C_6H_4Cl and L^- = S-*p*-C_6H_4Cl the abbreviations *p*Cl and S*p*Cl, respectively, are used.

In all cases the catecholate ligand is 3,6-diallylcatecholate, $(C_3H_5)_2$cat.

Preparation of Compounds. $(Et_4N)_4[M_2Fe_6S_8(SR)_6((C_3H_5)_2cat)_2]$ (**2**-Mo-Et, **2**-Mo-*p*Cl, **2**-W-Et)[5] and $(Et_4N)CN$[16] were synthesized by published methods. In the following preparations all operations were carried out under a pure dinitrogen atmosphere with degassed solvents.

(Et_4N)(S-*p*-C_6H_4Cl). To a solution of 66 mmol of sodium methoxide in 500 mL of methanol was added an equivalent amount (9.5 g) of *p*-chlorobenzenethiol and, within 5 min, 12 g (72 mmol) of Et_4NCl. After the mixture was stirred for 4 h the solvent was removed in vacuo. The oily residue was extracted with 300 mL of acetonitrile, the extract was filtered, and the filtrate volume reduced to ~50 mL. The white crystalline solid that separated upon cooling the solution at −20 °C for 16 h was collected by filtration and dried in vacuo: ^1H NMR (CD_3CN) anion δ 7.10 (2, d), 6.68 (2, d, J = 8.5 Hz); cation 3.18 (8, m), 1.19 (12, m).

(Et_4N)(OPh). To a suspension of 3.76 g (164 mmol) of sodium in 300 mL of diethyl ether was added 15.5 g (165 mmol) of phenol. The mixture was cooled in ice and was stirred overnight. Volume reduction to ~150 mL caused separation of a white solid, which was collected by filtration and washed with 30 mL of 1:1 v/v ether/*n*-hexane; 16.5 g (86%) of NaOPh was obtained. A solution of 11.6 g (70 mmol) of Et_4NCl in 120 mL of acetonitrile was added with stirring to a solution of 8.16 g (70 mmol) of NaOPh in 150 mL of THF. After the mixture was stirred overnight the cloudy solution was filtered (Celite pad), and the filtrate was concentrated to ~50 mL. Silky white needles separated on cooling the solution to −20 °C. This material was collected by filtration, washed with ether, and dried in vacuo, affording 8.1 g (52%) of product; ^1H NMR (CD_3CN) anion δ 6.79 (2, t, J = 8 Hz), 6.29 (2, d, J = 8 Hz), 6.01 (1, t, J = 6 Hz); cation 3.12 (8, m), 1.19 (12, m).

(Et_4N)$_4$[$W_2Fe_6S_8$(S-*p*-C_6H_4Cl)$_6$($(C_3H_5)_2$cat)$_2$] (2-W-*p*Cl). To a suspension of 6.60 g (2.97 mmol) of $(Et_4N)_4[W_2Fe_6S_8(SEt)_6((C_3H_5)_2cat)_2]$ in 250 mL of acetonitrile was added with stirring a solution of 2.73 g (18.9 mmol) of *p*-chlorobenzenethiol in 100 mL of acetonitrile The greenish-brown solution was filtered quickly; a crystalline solid appeared almost immediately after filtration. The filtrate was stirred for 4 h and cooled at −20 °C for 4 h. After collection by filtration, the solid was washed with ~200 mL of acetonitrile (40 °C) and dried in vacuo; 4.20 g (52%) of black crystals were obtained. Concentration of the filtrate wash and cooling afforded a second crop of 0.80 g (total yield 62%). Anal. Calcd for $C_{92}H_{128}Cl_6Fe_6N_4O_4S_{14}W_2$: C, 40.65; H, 4.75; Cl, 7.83; Fe, 12.33; N, 2.06; S, 16.51. Found: C, 40.63; H, 4.68; Cl, 7.69; Fe, 12.52; N, 2.02; S, 16.54.

(Et_4N)$_3$[$MoFe_3S_4$(S-*p*-C_6H_4Cl)$_4$($(C_3H_5)_2$cat)] (4-Mo-*pCl*-S*pCl*). $(Et_4N)_4[Mo_2Fe_6S_8(S\text{-}p\text{-}C_6H_4Cl)_6((C_3H_5)_2cat)_2]$ (0.800 g, 0.315 mmol) was dissolved in 180 mL of acetonitrile and the solution was filtered. To the filtrate was added a solution of 0.180 g (0.657 mmol) of (Et$_4$N)(S-*p*-C_6H_4Cl) in 20 mL of acetonitrile. After the reaction mixture was stirred for 30 min, its volume was reduced to ~20 mL. Slow addition of 25 mL of diethyl ether caused precipitation of a crystalline solid. This material was collected by filtration and dried in vacuo; 0.600 g (62%) of black needles was obtained: absorption spectrum (acetonitrile) λ_{max} 265 (ϵ_M 52 600), 306 (49 700), 364 (sh, 22 700), 436 (17 900) nm. Anal. Calcd for $C_{60}H_{88}Cl_4Fe_3MoN_3O_2S_8$: C, 46.64; H, 5.74; Cl, 9.18, Fe, 10.84; Mo, 6.21; N, 2.72; S, 16.60. Found: C, 46.60; H, 5.83; Cl, 9.31; Fe, 10.70; Mo, 5.99; N, 2.61; S, 16.48.

(Et_4N)$_3$[WFe_3S_4(S-*p*-C_6H_4Cl)$_4$($(C_3H_5)_2$cat)] (4-W-*p*Cl-S*pCl*). $(Et_4N)_4[W_2Fe_6S_8(S\text{-}p\text{-}C_6H_4Cl)_6((C_3H_5)_2cat)_2]$ (1.00 g, 0.368 mmol) was dissolved in 220 mL of acetonitrile and the solution was filtered. To the filtrate was added 0.213 g (0.777 mmol) of (Et$_4$N)(S-*p*-C_6H_4Cl) in 25 mL of acetonitrile. After the reaction mixture was stirred for 30 min, its volume was reduced to ~20 mL. Slow addition of diethyl ether initiated crystallization. The mixture was maintained at −20 °C for 20 h. The product was collected by filtration and dried in vacuo; 0.920 g (77%) of black crystals was obtained: absorption spectrum (acetonitrile) λ_{max} 264 (ϵ_M 50 800), 304 (48 600), 360 (sh, 24 900), 420 (19 750) nm. Anal. Calcd for $C_{60}H_{88}Cl_4Fe_3N_3O_2S_8W$: C, 44.13; H, 5.43; Cl, 8.68; Fe, 10.26; N, 2.57; S, 15.71. Found: C, 43.99; H, 5.40; Cl, 8.83; Fe, 10.18; N, 2.53; S, 16.11.

(13) Münck, E.; Rhodes, H.; Orme-Johnson, W. H.; Davis, L. C.; Brill, W. J.; Shah, V. K. *Biochim. Biophys. Acta* **1975**, *400*, 32.
(14) Huynh, B. H.; Münck, E.; Orme-Johnson, W. H. *Biochim. Biophys. Acta* **1979**, *527*, 192.
(15) Rawlings, J.; Shah, V. K.; Chisnell, J. R.; Brill, W. J.; Zimmerman, R.; Münck, E.; Orme-Johnson, W. H. *J. Biol. Chem.* **1978**, *253*, 1001.
(16) Webster, O. W.; Mahler, W.; Benson, R. E. *J. Am. Chem. Soc.* **1962**, *84*, 3678. Andreades, S.; Zahnow, E. W. *Ibid.* **1969**, *91*, 4181.

$(Et_4N)_3[MoFe_3S_4(S\text{-}p\text{-}C_6H_4Cl)_3((C_3H_5)_2cat)(CN)]$ (4-Mo-*p*Cl-CN). To a filtered solution of 0.800 g (0.315 mmol) of $(Et_4N)_4[Mo_2Fe_6S_8(S\text{-}p\text{-}C_6H_4Cl)_6((C_3H_5)_2cat)_2]$ in 200 mL of acetonitrile was added a solution of 0.100 g (0.640 mmol) of $(Et_4N)CN$ in 30 mL of acetonitrile. After the reaction mixture was stirred for 30 min, its volume was reduced to ~15 mL. The mixture was maintained at −20 °C for 40 h. The product was collected by filtration and dried in vacuo; 0.560 g (62%) of black crystals was isolated; IR (mull) ν_{CN} 2104 cm^{-1}. Anal. Calcd for $C_{55}H_{84}Cl_3Fe_3MoN_4O_2S_7$: C, 46.27; H, 5.93; Cl, 7.45; Fe, 11.74; Mo, 6.72; N, 3.92; S, 15.72. Found: C, 46.09; H, 5.88; Cl, 7.31; Fe, 11.77; Mo, 6.58; N, 3.96; S, 15.49.

$(Et_4N)_3[WFe_3S_4(S\text{-}p\text{-}C_6H_4Cl)_3((C_3H_5)_2cat)(CN)]$ (4-W-*p*Cl-CN). A procedure analogous to that of the preceding preparation was used. The volume of the reaction mixture was reduced to ~20 mL, and 25 mL of diethyl ether was added very slowly with stirring. The mixture was stored at −20 °C for 10 h. The product was collected by filtration and dried in vacuo; 0.480 g (54%) of black crystalline solid was obtained: IR (mull) ν_{CN} 2120 cm^{-1}. Anal. Calcd for $C_{55}H_{84}Cl_3Fe_3N_4O_2S_7W$: C, 43.59; H, 5.59; Fe, 11.06; N, 3.70; S, 14.81. Found: C, 43.50; H, 5.55; Fe, 10.85; N, 3.67; S, 14.93.

$(Et_4N)_3[MoFe_3S_4(SEt_3)_3((C_3H_5)_2cat)(CN)]$ (4-Mo-Et-CN). $(Et_4N)_4[Mo_2Fe_6S_8(SEt)_6((C_3H_5)_2cat)_2]$ (1.50 g, 0.733 mmol) was suspended in 100 mL of acetonitrile. To the suspension was added a solution of 0.250 g (1.60 mmol) of $(Et_4N)CN$ in 30 mL of acetonitrile with stirring. The solid slowly dissolved to give a clear red-brown solution, which was filtered and reduced in volume to ~20 mL. On slow addition of diethyl ether a crystalline solid was deposited. The material was collected by filtration and dried in vacuo, affording 1.20 g (69%) of black crystals: IR (mull) ν_{CN} 2100 cm^{-1}. Anal. Calcd for $C_{43}H_{87}Fe_3MoN_4O_2S_7$: C, 43.76; H, 7.43; Fe, 14.20; N, 4.75; S, 19.02. Found: C, 43.78; H, 7.50; Fe, 14.03; N, 4.91; S, 19.16.

$(Et_4N)_3[WFe_3S_4(SEt)_3((C_3H_5)_2cat)(CN)]$ (4-W-Et-CN). To a suspension of 1.50 g (0.67 mmol) of $(Et_4N)_4[W_2Fe_6S_8(SEt)_6((C_3H_5)_2cat)_2]$ in 150 mL of acetonitrile was added slowly with stirring a solution of 0.220 g (1.41 mmol) of $(Et_4N)CN$ in 50 mL of acetonitrile. The solid particles dissolved after stirring for 1 h. The solution was filtered and the filtrate was concentrated to ~20 mL. Slow addition of 40 mL of diethyl ether and cooling at −20 °C for 4 h caused separation of a solid, which was collected by filtration and dried in vacuo; 1.30 g (76%) of black needles was obtained: IR (mull) ν_{CN} 2100 cm^{-1}. Anal. Calcd for $C_{43}H_{87}Fe_3N_4O_2S_7W$: C, 40.73; H, 6.92; Fe, 13.21; N, 4.42; S, 17.70; W, 14.50. Found: C, 40.57; H, 6.87; Fe, 13.26; N, 4.66; S, 17.74; W, 14.39.

$(Et_4N)_3[MoFe_3S_4(S\text{-}p\text{-}C_6H_4Cl)_3((C_3H_5)_2cat)(OPh)]$ (4-Mo-*p*Cl-OPh). To a filtered solution of 1.00 g (0.393 mmol) of $(Et_4N)_4[Mo_2Fe_6S_8(S\text{-}p\text{-}C_6H_4Cl)_6((C_3H_5)_2cat)_2]$ in 200 mL of acetonitrile was added a solution of 0.200 g (0.895 mmol) of $(Et_4N)(OPh)$ in 25 mL of acetonitrile. After the reaction mixture was stirred for 30 min, its volume was reduced to ~20 mL and 15 mL of diethyl ether was added. This mixture was maintained at −20 °C for 20 h. Filtration of the product followed by drying in vacuo afforded 0.700 g (60%) of black crystalline solid. This compound has proven to be the least stable of the set 4-M-R-L and could not be obtained in high analytical purity. Anal. Calcd for $C_{60}H_{89}Cl_3Fe_3MoN_3O_3S_7$: C, 48.22; H, 6.00; Fe, 11.21; N, 2.81; S, 15.02. Found: C, 45.93; H, 5.78; Fe, 10.51; N, 2.72; S, 14.55. The ^1H NMR spectrum contained several weak impurity signals but otherwise was entirely consistent with the indicated formulation (see text).

$[MFe_3S_4(S\text{-}p\text{-}C_6H_4Cl)_3((C_3H_5)_2cat)(MeCN)]^{3-}$ (5-M-*p*Cl-MeCN). These clusters have been generated in solution by reduction of 4-M-*p*Cl-MeCN with sodium acenaphthylenide. Attempts to isolate their highly soluble Et_4N^+ salts have thus far been unsuccessful. Acetonitrile was distilled twice from CaH_2, THF was distilled from Na/K alloy and then from $LiAlH_4$, and acenaphthylene was sublimed twice under reduced pressure. A 0.40 M sodium acenaphthylenide stock solution was prepared by addition of 0.092 g (4.0 mmol) of finely divided sodium metal to a solution of 0.660 g (4.34 mmol) of acenaphthylene in 10.0 mL of THF, followed by stirring overnight. To a stirred solution of 11.8 μmol of $(Et_4N)_4[M_2Fe_6S_8(S\text{-}p\text{-}C_6H_4Cl)_6((C_3H_5)_2cat)_2]$ in 3.30 mL of acetonitrile was added 63 μL (25 μmol) of freshly prepared 0.4 M sodium acenaphthylenide solution, resulting in a color change from dark red-brown to dark green-brown. Formation of 5-M-*p*Cl-MeCN was essentially immediate and was monitored by changes in absorption spectra (see text).

$[MFe_3S_4(S\text{-}p\text{-}C_6H_4Cl)_3((C_3H_5)_2cat)L]^{3-}$ (6-M-*p*Cl-L, L = PEt_3, CO). Solutions of 5-M-*p*Cl-MeCN (~7 mM) were treated with the desired amount (mol ratio L:cluster ≥1) of ligand ($(Et_4N)(S\text{-}p\text{-}C_6H_4Cl)$, PEt_3, $(Et_4N)CN$, $PhCH_2NC$). In reactions with carbon monoxide (Matheson, 99.99%, passed through BASF catalyst and then Drierite), 3.3-mL solutions of ~7 mM 5-M-*p*Cl-MeCN were added to a 59-mL flask containing dinitrogen at 1 atm. Various volumes of the gas phase were removed corresponding to the desired number of equivalents of CO, which was then added at 1 atm. Reaction products were examined in situ by ^1H NMR spectroscopy and/or infrared spectroscopy.

Table I. Summary of Crystal Data, Intensity Collection, and Structure Refinement Parameters for $(Et_4N)_3[MoFe_3S_4(S\text{-}p\text{-}C_6H_4Cl)_4((C_3H_5)_2cat)]$

quantity	data
formula (M_r)	$C_{60}H_{88}Cl_4Fe_3MoN_3O_2S_8$ (1545.19)
a, Å	33.918 (8)
b, Å	16.674 (4)
c, Å	27.374 (5)
β, deg	95.98 (2)
crystal system	monoclinic
V, Å^3	15,396 (6)
Z	8
d_{calcd}, g/cm^3	1.33
d_{obsd},[a] g/cm^3	1.35
space group	$C2/c$
crystal dimensions, mm	0.40 × 0.60 × 0.63
radiation	Mo $K\bar{\alpha}$ (λ 0.710 69 Å)
absorption coefficient, μ, cm^{-1}	10.96
scan speed, deg/min	2.93 − 29.3 ($\theta/2\theta$ scan)
scan range, deg	2.4 + ($2\theta K\alpha_2 - 2\theta K\alpha_1$)
background/scan time ratio	0.25
data collected	2θ of 4.0 − 48.5°; $+h, +k, \pm l$
unique data ($F_o^2 > 2.5\sigma(F_o^2)$)	5511
no. of variables	752
goodness of fit	1.25
R, %	6.64
R_w, %	6.97

[a] Determined by flotation in CCl_4/cyclohexane.

X-ray Data Collection and Reduction. Clumps of large black crystals of $(Et_4N)_3[MoFe_3S_4(S\text{-}p\text{-}C_6H_4Cl)_4((C_3H_5)_2cat)]$ were obtained by slow diffusion of diethyl ether into an acetonitrile solution. A suitable crystal was cleaved from the mass and sealed in a glass capillary under an argon atmosphere. Diffraction experiments were performed with a Nicolet R3M four-circle automated diffractometer with a Mo X-ray tube equipped with a graphite monochromator. Data collection parameters are summarized in Table I. The orientation matrix and unit cell parameters were determined with 25 machine-centered reflections having $16.3 \leq 2\theta \leq 21.7°$. The crystal displayed symmetrical ω scans in the range 0.4−0.5°. The intensities of these standard reflections recorded after every 60 reflections were constant throughout the period of data collection. Data reduction and an empirical absorption correction were carried out with the program XTAPE of the SHELXTL structure determination package. The systematic absences hkl ($h + k \neq 2n$) and $h0l$ ($l \neq 2n$) are consistent with monoclinic space groups $C2/c$ and Cc. Statistical analysis of the diffracted intensities by the MULTAN subprogram NORMAL favored the centric space group. Solution and refinement of the structure confirmed space group $C2/c$. Crystal data are given in Table I.

Solution and Refinement of the Structure. The direct methods program MULTAN was employed. Trial positions for the Mo and Fe atoms were taken from the E map derived from the phase set with the highest combined figure of merit. Positions of the remaining non-hydrogen atoms were revealed in subsequent difference Fourier maps. The structure was refined by the blocked cascade least-squares method. Calculated fixed contributions from all hydrogen atoms (except those of cation 2) with thermal parameters set at 1.2 times that of the bonded carbon atom were included in the final refinement cycles. All non-hydrogen atoms were refined with anisotropic thermal parameters. The asymmetric unit consists of the anion and four cations, two of which have occupancies of 0.5. While two of the cations (3 and 4) are unexceptional, the third is equally distributed between two positions (1 and 2), one of which is on a 2-fold rotation axis (1) and the other is on an inversion center (2). Unique data used in the refinement and final R factor are given in Table I. The following results are tabulated: positional parameters (Table II) and interatomic distances and angles of the anion (Table III); thermal parameters of cations and anion (Table S-I); positional parameters of cations (Table S-II); unweighted least-squares planes of the anion (Table S-III); values of $10|F_o|$ and $10|F_c|$ (Table S-IV[17]).

(17) See paragraph at the end of this article concerning supplementary material.

Table II. Positional Parameters for $(Et_4N)_3[MoFe_3S_4(S\text{-}p\text{-}C_6H_4Cl)_4((C_3H_5)_2cat)]$

atom	x	y	z
Mo	0.34318 (3)[a]	0.06613 (5)	0.88605 (3)
Fe(1)	0.30520 (4)	0.0496 (1)	0.79342 (6)
Fe(2)	0.36657 (4)	−0.04861 (9)	0.82076 (6)
Fe(3)	0.37833 (4)	0.1093 (1)	0.80369 (5)
S(1)	0.40866 (8)	0.0353 (2)	0.8653 (1)
S(2)	0.30744 (8)	−0.0465 (2)	0.8523 (1)
S(3)	0.32345 (8)	0.1686 (2)	0.8288 (1)
S(4)	0.35597 (9)	0.0134 (2)	0.7473 (1)
S(5)	0.27812 (9)	0.1039 (2)	0.9231 (1)
S(6)	0.2524 (1)	0.0559 (2)	0.7347 (1)
S(7)	0.3913 (1)	−0.1727 (2)	0.8110 (1)
S(8)	0.4199 (1)	0.1879 (2)	0.7646 (1)
Cl(1)	0.1901 (2)	−0.1666 (4)	1.0297 (3)
Cl(2)	0.0929 (2)	0.1460 (6)	0.8177 (3)
Cl(3)	0.4340 (3)	−0.3436 (4)	1.0147 (3)
Cl(4)	0.4923 (3)	0.4658 (5)	0.9009 (4)
O(1)	0.3660 (2)	0.1570 (4)	0.9323 (2)
O(2)	0.3577 (2)	0.0060 (4)	0.9524 (2)
C(1)[b]	0.3755 (3)	0.1349 (7)	0.9786 (4)
C(2)	0.3696 (3)	0.0530 (6)	0.9906 (4)
C(3)	0.3783 (3)	0.0253 (7)	1.0388 (4)
C(4)	0.3924 (3)	0.0807 (8)	1.0744 (4)
C(5)	0.3988 (3)	0.1598 (7)	1.0631 (4)
C(6)	0.3913 (3)	0.1884 (7)	1.0152 (5)
C(7)	0.3728 (3)	−0.0639 (7)	1.0485 (4)
C(8)	0.3878 (4)	−0.0919 (9)	1.0985 (5)
C(9)	0.4119 (4)	−0.145 (1)	1.1106 (7)
C(10)	0.3975 (5)	0.2756 (8)	1.0025 (5)
C(11)	0.419 (1)	0.322 (1)	1.029 (1)
C(12)	0.432 (1)	0.377 (2)	1.043 (1)
C(1)S(5)	0.2536 (3)	0.0240 (6)	0.9495 (4)
C(2)S(5)	0.2156 (3)	0.0359 (8)	0.9607 (5)
C(3)S(5)	0.1948 (4)	−0.021 (1)	0.9845 (6)
C(4)S(5)	0.2137 (5)	−0.092 (1)	0.9976 (6)
C(5)S(5)	0.2520 (4)	−0.1069 (9)	0.9875 (5)
C(6)S(5)	0.2710 (3)	−0.0478 (7)	0.9627 (4)
C(1)S(6)	0.2091 (3)	0.0856 (7)	0.7602 (5)
C(2)S(6)	0.2051 (4)	0.0878 (7)	0.8107 (5)
C(3)S(6)	0.1698 (5)	0.1069 (9)	0.8272 (6)
C(4)S(6)	0.1367 (5)	0.124 (1)	0.7943 (8)
C(5)S(6)	0.1405 (5)	0.123 (1)	0.7459 (8)
C(6)S(6)	0.1761 (4)	0.1028 (9)	0.7279 (6)
C(1)S(7)	0.4021 (4)	−0.2190 (7)	0.8686 (5)
C(2)S(7)	0.3872 (4)	−0.1955 (8)	0.9123 (5)
C(3)S(7)	0.3975 (5)	−0.237 (1)	0.9558 (6)
C(4)S(7)	0.4231 (6)	−0.299 (1)	0.9564 (8)
C(5)S(7)	0.4367 (6)	−0.324 (1)	0.9166 (8)
C(6)S(7)	0.4276 (5)	−0.2825 (9)	0.8711 (7)
C(1)S(8)	0.4371 (5)	0.2638 (9)	0.8030 (6)
C(2)S(8)	0.4285 (6)	0.281 (1)	0.8474 (6)
C(3)S(8)	0.4402 (9)	0.342 (1)	0.8769 (8)
C(4)S(8)	0.468 (1)	0.390 (1)	0.864 (1)
C(5)S(8)	0.481 (1)	0.376 (2)	0.818 (1)
C(6)S(8)	0.460 (1)	0.321 (2)	0.786 (1)

[a] Estimated standard deviations in parentheses in this and succeeding tables. [b] Labeling schemes for the S-*p*-C_6H_4Cl and diallylcatechol ligands:

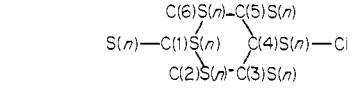

(n = 5–8)

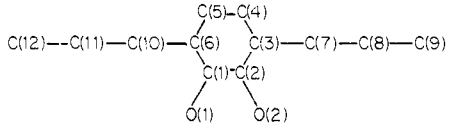

Other Physical Measurements. All measurements were performed under anaerobic conditions. Spectroscopic (electronic absorption, 300-MHz ^1H NMR, X-band EPR) and electrochemical properties were determined with instrumentation described previously.[3,5] Infrared spectra were measured with a Perkin-Elmer 599B spectrophotometer. Chemical shifts of the paramagnetic clusters which are upfield and downfield of Me_4Si reference are designated as positive and negative, respectively. Potentials were measured by cyclic voltammetry (100 mV/s) at ~25 °C vs. a saturated calomel electrode (SCE) as reference.

Table III. Selected Interatomic Distances (Å) and Angles (deg) in $[MoFe_3S_4(S\text{-}p\text{-}C_6H_4Cl)_4((C_3H_5)_2cat)]^{3-}$

Mo–S(1)	2.405 (3)	Fe(1)···Fe(2)	2.693 (2)[a]
Mo–S(2)	2.370 (3)[a]	Fe(1)···Fe(3)	2.660 (2)[a]
Mo–S(3)	2.367 (3)[a]	Fe(2)···Fe(3)	2.711 (2)
mean	2.38 (2)[e]	mean	2.69 (3)
Mo···S(4)	3.968 (3)	Fe(1)···S(1)	3.848 (3)
Mo–S(5)	2.600 (3)	Fe(2)···S(3)	3.920 (3)[a]
Mo–O(1)	2.073 (7)	Fe(3)···S(2)	3.868 (3)[a]
Mo–O(2)	2.087 (6)	mean	3.88 (4)
mean	2.080	O(1)···O(2)	2.599 (9)
Fe(1)–S(2)	2.267 (3)[a]	S(1)···S(2)	3.677 (4)[a]
Fe(1)–S(3)	2.265 (3)[a]	S(1)···S(3)	3.700 (4)[a]
Fe(1)–S(4)	2.320 (4)	S(1)···S(4)	3.545 (4)
Fe(2)–S(1)	2.263 (3)[b]	S(2)···S(3)	3.693 (4)
Fe(3)–S(1)	2.250 (3)[b]	S(2)···S(4)	3.599 (4)[b]
Fe(2)–S(2)	2.264 (3)[c]	S(3)···S(4)	3.661 (4)[b]
Fe(3)–S(3)	2.276 (3)[c]	mean	3.65 (6)
Fe(2)–S(4)	2.258 (3)[d]	Mo–S(1)–Fe(2)	73.3 (1)[a]
Fe(3)–S(4)	2.297 (3)[d]	Mo–S(1)–Fe(3)	72.5 (1)[a]
mean	2.27 (2)	Mo–S(2)–Fe(1)	72.3 (1)[b]
Fe(1)–S(6)	2.281 (3)	Mo–S(3)–Fe(1)	72.4 (1)[b]
Fe(2)–S(7)	2.259 (4)[a]	Mo–S(2)–Fe(2)	74.0 (1)[c]
Fe(3)–S(8)	2.272 (4)[a]	Mo–S(3)–Fe(3)	72.7 (1)[c]
mean	2.271 (11)	mean	72.9
C(1)S(5)–S(5)	1.77 (1)	O(1)–Mo–S(2)	164.0 (2)
C(1)S(6)–S(6)	1.76 (1)	O(2)–Mo–S(3)	161.3 (2)
C(1)S(7)–S(7)	1.76 (1)	S(1)–Mo–S(5)	170.5 (1)
C(1)S(8)–S(8)	1.71 (2)	Fe(1)–S(2)–Fe(2)	72.9 (1)[a]
mean	1.75 (3)	Fe(1)–S(3)–Fe(3)	71.7 (1)[a]
C(1)–O(1)	1.33 (1)	Fe(1)–S(4)–Fe(2)	72.1 (1)[b]
C(2)–O(2)	1.34 (1)	Fe(1)–S(4)–Fe(3)	70.4 (1)[b]
mean	1.34	Fe(2)–S(1)–Fe(3)	73.8 (1)
O(1)–Mo–O(2)	77.3 (3)	Fe(2)–S(4)–Fe(3)	73.1 (1)
O(1)–Mo–S(1)	90.3 (2)	mean	72.3
O(1)–Mo–S(3)	86.5 (2)	Fe(1)–Mo–Fe(2)	58.3 (1)[a]
O(1)–Mo–S(5)	82.1 (2)	Fe(1)–Mo–Fe(3)	58.0 (1)[a]
O(2)–Mo–S(1)	87.9 (2)	Fe(2)–Mo–Fe(3)	58.6 (1)
O(2)–Mo–S(2)	91.3 (2)	mean	58.3
O(2)–Mo–S(5)	84.8 (2)	S(2)–Fe(1)–S(3)	109.1 (1)
S(1)–Mo–S(2)	100.7 (1)	S(2)–Fe(1)–S(4)	103.4 (1)[a]
S(1)–Mo–S(3)	101.7 (1)	S(3)–Fe(1)–S(4)	106.0 (1)[a]
S(2)–Mo–S(3)	102.4 (1)	S(1)–Fe(2)–S(2)	108.6 (1)[b]
S(2)–Mo–S(5)	85.6 (1)[a]	S(1)–Fe(3)–S(3)	109.6 (1)[b]
S(3)–Mo–S(5)	83.7 (1)[a]	S(1)–Fe(2)–S(4)	103.3 (1)[c]
Mo···Fe(1)	2.736 (2)	S(1)–Fe(3)–S(4)	102.5 (1)[c]
Mo···Fe(2)	2.789 (2)[a]	S(2)–Fe(2)–S(4)	105.5 (1)[d]
Mo···Fe(3)	2.754 (2)[a]	S(3)–Fe(3)–S(4)	106.4 (1)[d]
mean	2.76 (3)	mean	106.0

[a-d] Superscripts designate symmetry-related dimensions under idealized C_s symmetry of the $MoFe_3S_4$ core unit. [e] The standard deviation of the mean was estimated as $\sigma \approx s = [(\Sigma x_i^2 - n\bar{x}^2)/(n-1)]^{1/2}$.

Results and Discussion

Some seven clusters of the type **4**-M-R-L (R = *p*Cl, Et; L^- = S*p*Cl, CN, OPh) have been isolated from reaction 4, in which the solvate clusters **3**-M-R-MeCN,[5] generated by reaction 2 in acetonitrile solution, were treated with a small excess (≤12%) of the ligands L^-. Use of the substituent R = *p*Cl results in decreased solubility compared to R = Ph or Et and the formation of highly crystalline solids, the structure of one of which has been determined by X-ray diffraction methods.

Structure of $(Et_4N)_3[MoFe_3S_4(S\text{-}p\text{-}C_6H_4Cl)_4((C_3H_5)_2cat)]$. This compound crystallizes in monoclinic space group $C2/c$, and its crystal structure consists of discrete cations and anions. Structural features of the cations and the organic portions of the anion are unexceptional and are not considered. The structure of the anion (briefly described earlier[4]) is shown in Figure 2 and a stereoview of a different orientation is provided in Figure 3. The shortest

Table IV. ^1H Chemical Shifts (ppm, ~297 K) of Clusters in CD_3CN Solutions

cluster	*m*-H Fe(1)[a]	*m*-H Fe(2,3)	*o*-H Fe(1)	cat-H	other
3-Mo-*p*Cl-MeCN	−13.3[f]		2.69[f]	−9.35	
3-Mo-Et-Me_2SO[d]				−10.1	−49[b] (CH_2), −3.8[c] (CH_3)
3-W-*p*Cl-MeCN	−13.1[f]		1.58[f]	−9.15	
3-W-Et-Me_2SO[d]				−8.95	−47[b] (CH_2), −4.09 (CH_3)
4-Mo-*p*Cl-S*p*Cl	−17.6	−10.5	9.84	−10.7	−7.3[c] (*o*-H, Mo), −7.12 (*m*-H, Mo)
4-Mo-*p*Cl-CN	−17.8	−10.6	9.40	−10.6	
4-Mo-Et-CN				−10.4	−88[b] (CH_2, Fe(1)), −28.5 (CH_2, Fe(2,3))
4-Mo-*p*Cl-OPh	−18.0	−10.4	~10[b]	−10.7	−7.5[c] (*o*-H, Mo), −7.09 (*m*-H, *p*-H, Mo)
4-Mo-*p*Cl-PEt_3	−19.3	−10.3	9.30	−10.5	−8.2[b] (PCH_2), −2.52 (PCH_2CH_3)
4-W-*p*Cl-S*p*Cl	−17.2	−10.6	7.91	−9.48	−7.07 (*o*-H, Mo), −6.79 (*m*-H, Mo)
4-W-*p*Cl-CN	−16.9	−11.0	7.32	−9.35	
4-W-Et-CN				−9.15	−79[b] (CH_2, Fe(1)), −30.7, −29.7 (CH_2, Fe(2,3))
5-Mo-*p*Cl-MeCN	−16.4[f]		4.65[f]	−4.54	
5-W-*p*Cl-MeCN	−16.3[f]		3.38	−4.58	
6-Mo-*p*Cl-PEt_3	−20.6	−14.2	10.2	−11.0	−10.4[b] (PCH_2)
6-W-*p*Cl-PEt_3	−20.2	−14.1	*e*	−9.28	−9.2[b] (PCH_2)

[a] Atoms numbered as in Figure 2. [b] Very broad signal. [c] Shoulder. [d] Me_2SO solvate; compound sparingly soluble in acetonitrile. [e] Not located. [f] One resonance observed for all Fe-S*p*Cl ligands.

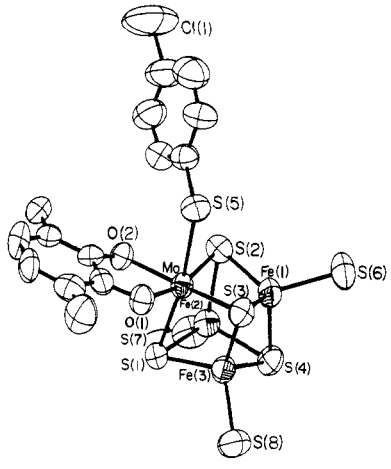

Figure 2. Structure of $[MoFe_3S_4(S\text{-}p\text{-}C_6H_4Cl)_4((C_3H_5)_2cat)]^{3-}$ (**4**-Mo-*p*Cl-S*p*Cl), showing 50% probability ellipsoids and the atom labeling scheme. The $p\text{-}C_6H_4Cl$ and vinyl groups of the Fe–thiolate and catecholate ligands, respectively, are omitted.

intercluster metal–metal distance is 9.05 Å, between symmetry-related Fe(3) atoms. The closest intercluster Mo···Fe and Mo···Mo approaches are 10.5 Å and 11.2 Å, respectively. Hence **4**-Mo-*p*Cl-S*p*Cl is the first structurally proven case of a MFe_3S_4 single cubane, i.e., a cluster not bridged to a second cluster (as in, e.g., **1**-M[8] and $[M_2Fe_6S_8(SR)_9]^{3-}$,[5-3,7,10,18]) or having an appended paramagnetic fragment.[11] Other claims of $MoFe_3S_4$ single cubanes[19,20] are not sustained by the evidence presented.

The cluster **4**-Mo-*p*Cl-S*p*Cl contains a cubane-type $MoFe_3S_4$ core composed of two interpenetrating, imperfect $MoFe_3$ and S_4 tetrahedra. Each Fe atom is terminally coordinated by one thiolate ligand and occupies an approximately tetrahedral site. Molybdenum atom coordination external to the core is completed by a chelating catecholate group and a thiolate ligand. The metrical features of the anion, compiled in Table III, are quite similar to those of the subclusters in $[Mo_2Fe_6S_8(SEt)_6(3,6\text{-}(n\text{-}Pr)_2cat)_2]^{4-}$ (**2**-Mo), whose structure has been described.[5] The principal structural features of **4**-Mo-*p*Cl-S*p*Cl are briefly summarized. (i) There is no imposed symmetry, a matter immediately apparent from the spatial disposition of the Mo-S*p*Cl ligand (Figure 3). (ii) The highest idealized symmetry of the $MoFe_3S_4$ core and of the cluster (excluding *p*Cl and allyl groups) is C_s. Cores of clusters with approximate (or exact) trigonal symmetry at the Mo atom are well described under C_{3v} symmetry.[3,7,8,18] This is not the case here; core dimensions reflect the presence of mixed ligands external to the core. For example, among bonded distances Mo–S(1) (2.405 (3) Å) and Fe(1)–S(4) (2.320 (4) Å) are elongated compared to other members of their sets, and emphasize departure from trigonal symmetry.[21] The C_s symmetry description is of course not exact because distances and angles related under this symmetry (Table III) are not equal, and in several instances the inequalities are large (e.g., Fe(2)–S(4), 2.258 (3) Å; Fe(3)–S(4), 2.297 (3) Å).[22] (iii) The six core faces are nonplanar rhombs with Mo, Fe, and S atom positional deviations from unweighted least-squares planes being ±(0.14–0.19) Å, except for the plane Fe(2)Fe(3)S(1)S(4) where the deviations are larger and regular (±0.20 Å). Diagonal quadrilaterals are nearly perfectly planar (deviations of ≤(±0.01) Å[17]). (iv) The Mo–S(5) distance of 2.600 (3) Å is 0.05–0.09 Å shorter than the Mo–S distances in the Mo(μ_2-S)Fe bridges of three structures of the clusters **2**-Mo.[5,12] The mean of the Fe–S(6–8) bond lengths, 2.27 (2) Å, is the same as that of the terminal Fe–S, and is 0.04–0.06 Å shorter than the bridge Fe–S, distance in **2**-Mo. These results show that bridge bonds in the latter clusters are somewhat elongated compared to terminal ones. This property presumably contributes to the ready occurrence of reaction 2, in which bridging thiolates are converted to terminal ligands. (v) The Mo atom coordination site is a severely distorted octahedron, with angles involving mutually cis ligand atoms in the range 77–102°.

Solution Structure of Clusters 4-M. With establishment of the single-cubane structure of **4**-Mo-*p*Cl-S*p*Cl in the solid state, which presumably applies to the entire set of crystallized salts containing the clusters **4**-M-R-L, the structures of these clusters in acetonitrile solution have been investigated by ^1H NMR spectroscopy. Spectra of four members of the set are presented in Figures 4 and 5. Resonances of all clusters **3**-M-R-solv and **4**-M-R-L are isotropically shifted[23] as a consequence of their $S = {}^3/_2$ ground

(18) Christou, G.; Garner, C. D.; Mabbs, F. E.; King, T. J. *J. Chem. Soc., Chem. Commun.* **1978**, 740. Christou, G.; Garner, C. D.; Miller, R. M.; King, T. J. *J. Inorg. Biochem.* **1979**, *11*, 349.

(19) Otsuka, S.; Kamata, M. In "Molybdenum Chemistry of Biological Significance"; Newton, W. E.; Otsuka, S., Eds.; Plenum Press: New York, 1980; pp 229–238.

(20) Ungurenasu, C.; Cotzur, C.; Harabagiu, V. *Polym. Bull.* **1980**, *2*, 521.

(21) The corresponding long Fe(1)–S(4) distance of 2.311 (3) Å in the subclusters of $[Mo_2Fe_6S_8(SEt)_6(3,6\text{-}(n\text{-}Pr)_2cat)_2]^{4-}$ (**2**-Mo) can no longer be associated, as was proposed,[5] with strain in the core owing to the involvement of the Fe(1) atom in a Fe(μ_2-SEt)Mo bridge. This longer bond is a property of $MoFe_3S_4$ cubanes with effective or real C_s symmetry.

(22) An example of exact C_s symmetry is found with the recently prepared compound $(Et_4N)_2[MoFe_3S_4Cl_3((C_3H_5)_2cat)(THF)]$, in which the cluster has a crystallographically imposed mirror plane (Palermo, R. E.; Holm, R. H., results to be published).

(23) $(\Delta H/H_0)_{iso} = (\Delta H/H_0)_{obsd} - (\Delta H/H_0)_{dia}$, where the diamagnetic reference shifts are those of the free ligands. The data in Table IV are the chemical (i.e., observed) shifts inasmuch as no analysis of isotropic shifts is included here. Considerations of isotropic shifts of MFe_3S_4-type clusters are available elsewhere.[3,9,10]

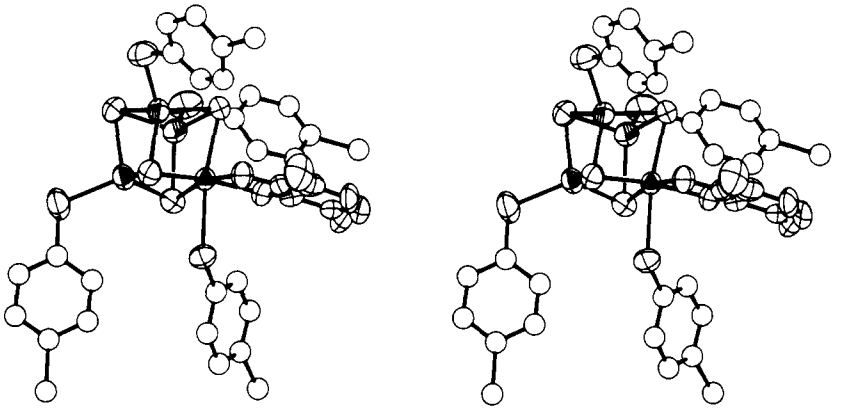

Figure 3. Stereoview of the structure of cluster in Figure 2 from a different orientation (vinyl groups of the catecholate ligand are omitted).

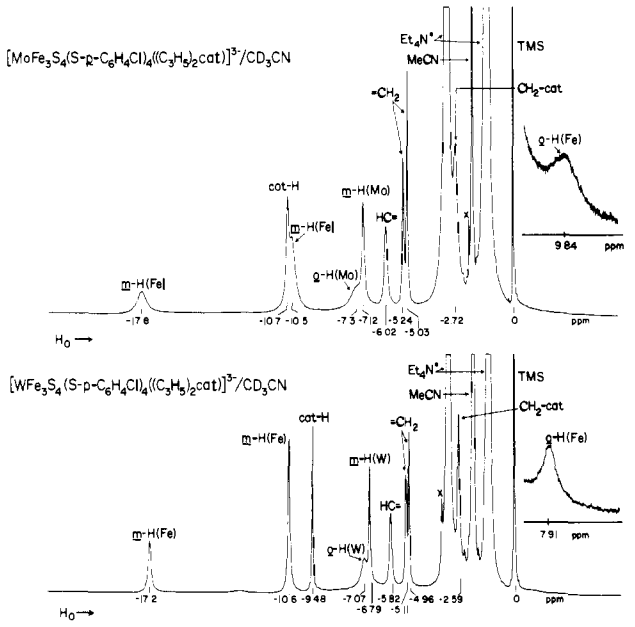

Figure 4. ^{1}H NMR spectra (300 MHz, ~297 K) of ~10 mM solutions of 4-Mo-*p*Cl-S*p*Cl (upper) and 4-W-*p*Cl-S*p*Cl (lower) in CD_3CN. Signal assignments are indicated (x = impurity).

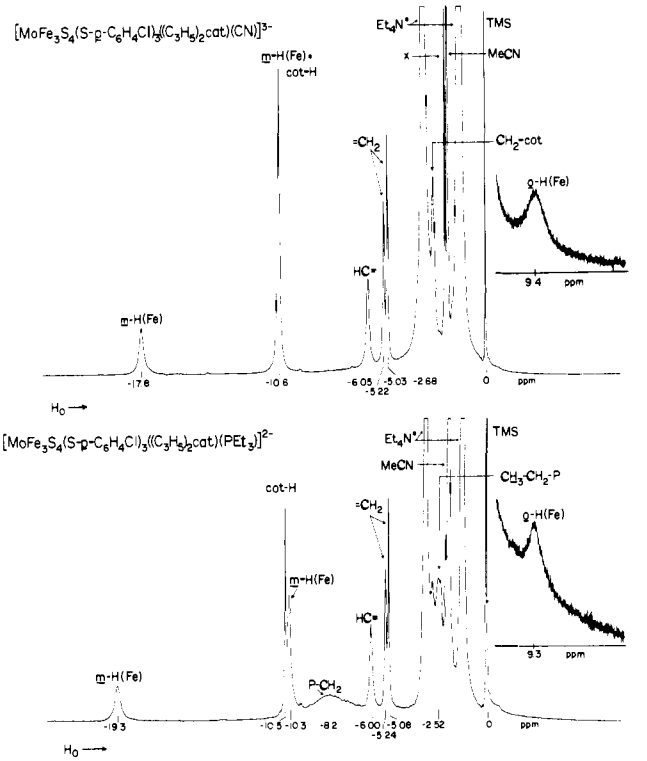

Figure 5. ^{1}H NMR spectra (300 MHz, ~297 K) of ~10 mM solutions of 4-Mo-*p*Cl-CN (upper) and 4-Mo-*p*Cl-PEt_3 (lower) in CD_3CN. Signal assignments are indicated (x = impurity).

states[1,4,5] (vide infra). Chemical shifts of solvated and ligated clusters, excluding those of allyl groups of the $(C_3H_5)_2$cat ligands, are collected in Table IV.[23] In all cases the assignment of catecholate (cat-H) resonances is based on the spectra of solvated cluster precursors containing the $(C_3H_5)_2C_6D_2O_2$ ligand[5] and relative signal intensities of the ligated clusters.

The most significant spectral feature of the set 4-M-R-L is the appearance of two CH_2 (R = Et) and two *m*-H (R = *p*Cl) resonances of Fe-bound terminal ligands. In the spectra of 4-M-*p*Cl-S*p*Cl (Figure 4) the *m*-H signals occur near −17 and −10 ppm in an intensity ratio of 1:2. Narrower line widths and enhanced resolution are consistent features of the spectra of M = W clusters compared to their M = Mo analogoues. Corresponding features are illustrated in the spectra of 4-Mo-*p*Cl-CN and 4-Mo-*p*Cl-PEt_3 (Figure 5). In the former case spectra at ~250 K reveal two signals near −11 ppm in a 2:1 intensity ratio, consistent with the indicated assignments. The chemical shift separation between the two types of CH_2 groups in 4-M-Et-CN is strikingly large and is ~60 ppm in the M = Mo cluster. The spectra of all clusters 4-M-*p*Cl-L exhibit one broad *o*-H resonance of Fe-SR ligands at 7–10 ppm. For 4-Mo-Ph-SPh, formed in solution by reaction 4, the Fe-SPh ligands afford a single *p*-H feature at 10.5 ppm with one-half of the intensity of the *m*-H signal at −17.5 ppm. These observations lead to the conclusion that the remaining *o*-H and *p*-H resonances, necessarily associated with the ligands having the smaller *m*-H isotropic shift (chemical shifts of ~−10 ppm), are themselves less shifted and are obscured by cation and solvent absorptions.

Variation of ligand L in the set 4-Mo-*p*Cl-L results in only small changes in the chemical shifts of *p*Cl resonances. Consequently, resonances of the ligands L = S*p*Cl and OPh bound to the Mo atom are readily assigned by comparison with the spectra of L = CN clusters (Figures 4 and 5). Their most conspicuous feature is that of small (<1 ppm) isotropic shifts.[23]

The presence of two *m*-H and two CH_2 resonances of Fe-SR ligands, together with one cat-H and one set of L = S*p*Cl, OPh signals, is fully consistent with cluster structures of effective C_s symmetry in solution. The Fe-SR resonances of relative intensities 2:1 must be associated with ligands bound to Fe(2,3) and Fe(1), respectively (Figure 2). The origin of the larger isotropic shifts associated with Fe(1), lying in the mirror plane, is not presently understood. The chemical shifts of the anisochronous methylene protons of Fe(2,3)-SEt groups differ by 1.0 ppm in the spectrum of 4-W-Et-CN. Resonances of these protons are not resolved in the spectrum of 4-Mo-Et-CN. The methylene protons of Fe(1)-SEt groups are isochronous under C_s symmetry and only one (broad) signal was observed in each case. The spectra of members

Table V. Redox Potentials[a] of Clusters

cluster	E_1, $[MFe_3S_4]^{3+/2+}$[b] Mo	E_1, $[MFe_3S_4]^{3+/2+}$[b] W	E_2, $[MFe_3S_4]^{4+/3+}$[b] Mo	E_2, $[MFe_3S_4]^{4+/3+}$[b] W
3-M-*p*Cl-MeCN	−1.02	−1.22	−0.08	−0.17
3-M-*p*Cl-DMF[c]	−1.12	−1.30	−0.20	−0.28
3-M-*p*Cl-Me_2SO[d]	−1.08	−1.27	(−0.11)[e]	(−0.12)[e]
3-M-Et-Me_2SO[d]	−1.33	−1.53	−0.35	−0.45
4-M-*p*Cl-S*p*Cl	−1.07	−1.27	(−0.36)[e]	(−0.43)[e]
4-M-*p*Cl-CN	−1.30	−1.45	−0.24	−0.32
4-M-Et-CN	−1.60	−1.77	−0.54	−0.63
4-M-*p*Cl-OPh	−1.10		(−0.29)[e]	
4-M-*p*Cl-PEt_3	−1.18		−0.13	
(4-M-*p*Cl)$_2$dmpe	−1.13		−0.11	

[a] E(V) = $(E_{p,c} + E_{p,a})/2$ (100 mV/s) vs. SCE; acetonitrile solution unless noted otherwise. [b] Core oxidation levels; cf. series (eq 6) (text). [c] DMF solution. [d] Me_2SO solution. [e] $E_{p,a}$; irreversible.

of the **4**-M-R-L set are to be contrasted with those of the clusters **3**-M-R-solv, which have been extensively studied earlier.[5] All solvated clusters exhibit a single set of R group resonances in acetonitrile, Me_2SO, and DMF solutions over the range 250–350 K. In these species Fe site inequivalencies are averaged by rapid exchange of bound and bulk solvent accompanied by a degenerate reorientation of the catecholate ligand, affording effective C_{3v} cluster symmetry on the NMR time scale. This interpretation is supported by the observation that the *m*-H shifts of solvated clusters are close to the weighted averages of the shifts of ligated clusters (e.g., −13.3 ppm for **3**-Mo-*p*Cl-MeCN vs. −13.0 ppm for **4**-Mo-*p*Cl-CN). Similarly, the *o*-H shift (2.69 ppm) of **3**-Mo-*p*Cl-MeCN together with the Fe(1) *o*-H shift (9.40 ppm) of **4**-Mo-*p*Cl-CN leads to the prediction that the Fe(2,3) *o*-H signal of the latter cluster should occur near −0.7 ppm. As noted above this (broad) signal is presumably obscured by other resonances in that region (cf. Figure 5). Corresponding estimates for other **4**-M-*p*Cl-L clusters place the unobserved *o*-H signals in the same region.

The 2:1 intensity pattern of Fe-SR resonances serves as a simple indicator of complex formation by an added ligand L in the absence of fast exchange. Of the preceding three solvents acetonitrile forms the most, and Me_2SO the least, substitutionally labile clusters. The isolated clusters **4**-M-*p*Cl-L (L^- = S*p*Cl, OPh, CN) are stable in acetonitrile but, except for the cyanides, are completely dissociated in Me_2SO. Addition of 1.0 equiv of PEt_3 to a ~10 mM solution of **3**-Mo-*p*Cl-MeCN results in quantitative formation of **4**-Mo-*p*Cl-PEt_3 whose spectrum, indicative of C_s symmetry, has already been noted. By similar means a linked double cubane (**4**-Mo-*p*Cl)$_2$(dmpe) was formed from 2.0 equiv of **3**-Mo-*p*Cl-MeCN and 1.0 equiv of $Me_2PCH_2CH_2PMe_2$ (dmpe). Its *m*-H and cat-H shifts are essentially identical with those of the PEt_3 adduct. Lastly, while 40 mM **4**-Mo-Ph-SPh (*m*-H, −17.5 (1), −10.6 (2) ppm) is stable in acetonitrile, addition of as little as 10 equiv of Me_2SO produces detectable amounts of **3**-Mo-Ph-Me_2SO and 200 equiv causes complete conversion to the solvated cluster (*m*-H, −13.1; cat-H, −10.5; *p*-H, 3.07 ppm). On the basis of these results, studies of reduced clusters have been conducted in acetonitrile in order to minimize ligand dissociation.

Reduced Clusters 5-M and 6-M. (a) Formation. Previously it has been shown that the solvated clusters **3**-M undergo a one-electron reduction in Me_2SO solution[5] and that several ligated clusters sustain one-electron oxidation and reduction reactions in acetonitrile solution.[4] Further cyclic voltammetric studies have established the three-membered electron transfer series (eq 6),

$$\underset{\substack{\textbf{5}\text{-M-R-solv}\\ \textbf{6}\text{-M-R-L}}}{[MFe_3S_4]^{2+}} \overset{E_1}{\rightleftharpoons} \underset{\substack{\textbf{3}\text{-M-R-solv}\\ \textbf{4}\text{-M-R-L}}}{[MFe_3S_4]^{3+}} \overset{E_2}{\rightleftharpoons} [MFe_3S_4]^{4+} \qquad (6)$$

described in terms of $[MFe_3S_4]$ core oxidation levels. Values of the potentials E_1 and E_2 in acetonitrile solutions are collected in Table V; representative cyclic voltammograms are presented elsewhere.[4,5] Greater interest attends the reduction reactions (E_1)

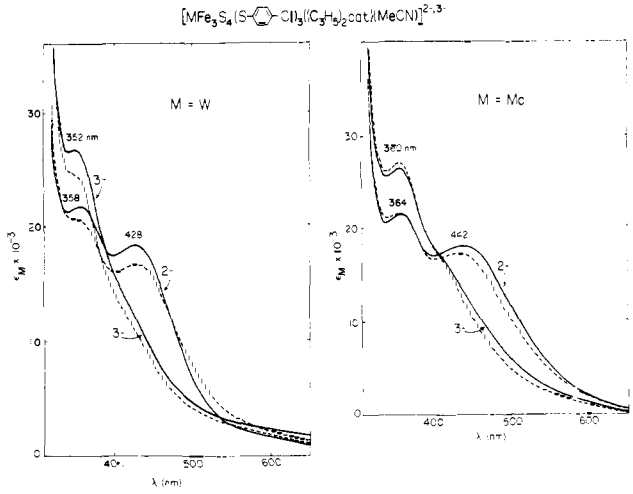

Figure 6. Absorption spectra of **3**-M-*p*Cl-MeCN (2-) and **5**-M-*p*Cl-MeCN (3-) in acetonitrile solutions. The reduced species were generated in an OTTLE cell at applied potentials of −1.30 V (Mo) and −1.55 V (W). (−) oxidized and initially reduced species; (- -) reoxidized and rereduced species. The elapsed time between recording of the first (oxidized) and last (reduced) spectra was 150 min.

inasmuch as the reduced clusters are those which are more likely to bind and activate reducible substrates. All such reactions are chemically reversible ($i_{p,c}/i_{p,a} \simeq 1$) for solvated and phosphine-ligated clusters. For the species **4**-M-R-L containing anionic ligands, this situation is closely approached, but small quantities of solvated clusters are detectable in anodic scans after generation of **6**-M-R-L, indicating a slight extent of ligand dissociation in the reduced clusters. Two regularities of reversible potentials are evident: ΔE_1(Mo–W) = 0.15–0.20 V and ΔE_2(Mo–W) = 0.08–0.09 V at parity of R and solvent or L; $\Delta E_{1,2}$(*p*Cl-Et) = 0.25–0.32 V when only R is varied. More negative potentials for tungsten members of pairs of analogous Mo/W complexes is the usual situation,[4,9,24] and the R substituent dependence parallels that observed with MFe_3S_4 double cubanes.[3,24b] The second of these regularities supports assignment of the potential E_2 to a process best described as core-based rather than to a redox reaction centered on the $(C_3H_5)_2$cat ligand. The latter type of reaction has been documented in Mo–catecholate complexes.[25] Clusters containing the 4+ core oxidation level have been detected only by electrochemical means and are not considered further.

Inasmuch as attempts to isolate reduced clusters have been unsuccessful,[26a] several experiments were performed to obtain diagnostic criteria for their formation. The results of spectroelectrochemical experiments on the clusters **3**-M-*p*Cl-MeCN are presented in Figure 6. These clusters were caused to traverse two redox cycles by using applied potentials sufficient to effect complete electron transfer in a given step. Spectra of the reduced clusters **5**-M-*p*Cl-MeCN lack the prominent 442-nm (Mo) or 428-nm (W) maxima of the oxidized species. The spectrum of 5-Mo-*p*Cl-MeCN is quite similar to that of the reduced, fully characterized double cubane $[Mo_2Fe_6S_8(SPh)_9]^{5-,3}$ whose subclusters are isoelectronic with the single-cubane species. Reoxidation of the initially reduced clusters results in recovery of the original spectra but with 4.6% (Mo) and 8.5% (W) intensity decreases at the visible maxima. Rereduction afforded spectra

(24) (a) Taylor, R. D.; Street, J. P.; Minelli, M.; Spence, J. T. *Inorg. Chem.* **1978**, *17*, 3207. Rice, C. A.; Kroneck, P. H. M.; Spence, J. T. *Ibid.* **1981**, *20*, 1996. Bradbury, J. R.; Masters, A. F.; McDonell, A. C.; Brunette, A. A.; Bond, A. M.; Wedd, A. G. *J. Am. Chem. Soc.* **1981**, *103*, 1959. (b) For an apparent exception to this behavior cf.: Christou, G.; Garner, C. D.; Miller, R. M.; Johnson, C. E.; Rush, J. D. *J. Chem. Soc., Dalton Trans.* **1980**, 2363.

(25) Pierpont, C. G.; Buchanan, R. M. *Inorg. Chem.* **1982**, *21*, 652; *Coord. Chem. Rev.* **1981**, *38*, 45.

(26) (a) **Note Added in Proof**: Reduced clusters have now been isolated and exhibit the same spectroscopic properties as those described here for species generated in situ. (b) Reynolds, J. G.; Laskowski, E. J.; Holm, R. H. *J. Am. Chem. Soc.* **1978**, *100*, 5315.

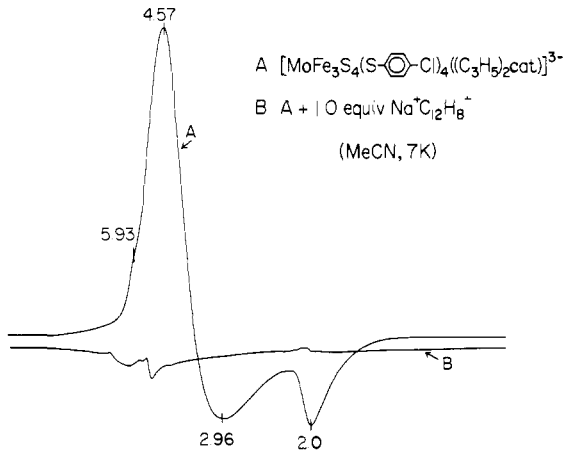

Figure 7. X-band EPR spectra at 7 K in acetonitrile solution: A, **4**-Mo-*p*Cl-S*p*Cl; B, after addition of 1.0 equiv of sodium acenaphthylenide in THF to A. Instrument settings are the same for both spectra.

somewhat less intense than those of the initially generated reduced clusters. It is evident that over the time period (150 min) of the two redox cycles the individual steps are not completely reversible and that the Mo clusters are the more stable to electron transfer. The spectra obtained in the first reductions have been taken as the absorption spectral criteria for complete formation of the clusters **5**-M-*p*Cl-MeCN in all subsequent experiments involving generation of these species by the chemical reduction reaction 5. Treatment of **3**-M-*p*Cl-MeCN with a 6% excess of sodium acenaphthylenide in THF affords absorption spectra that, after allowance for the organic chromophores, are indistinguishable from the criterion spectra. As a further check on the occurrence of a one-electron reduction reaction a solution of **4**-Mo-*p*Cl-S*p*Cl in acetonitrile was treated with 1.0 equiv of sodium acenaphthylenide in THF. EPR spectra before and after reaction are shown in Figure 7. The spectrum of the initial species is entirely typical of those of solvated and ligated clusters[1,4,5] and corresponds to a rhombic $S = {}^3/_2$ spin system. The reaction product is EPR-silent, indicating the formation of a $S = 0$ or even species.

(b) Solvated Clusters. Triplicate reductions of **3**-Mo-*p*Cl-MeCN by reaction 5 afforded NMR spectra that were unchanged over periods of at least 40 h and whose shifts were consistent to ±0.01 ppm, observations indicative of reproducible generation of a stable reduced cluster. The species **5**-W-*p*Cl-MeCN was generated analogously. The spectrum of **5**-Mo-*p*Cl-MeCN, displayed in Figure 8, contains one set of *o*-H and *m*-H resonances, demonstrating that the property of rapid exchange of bound and bulk solvent molecules extends to the reduced clusters as well. The most characteristic spectral feature is the shift of the cat-H resonance (verified by deuteration) from ~−9 ppm in the oxidized clusters to −4.5 ppm in the reduces species. Several weak impurity signals are observed, including the *m*-H resonances of $[Fe_4S_4(SpCl)_4]^{3-}$ (−10.8 ppm, assigned by analogy with the shift of $[Fe_4S_4(SPh)_4]^{3-}$[26b]). Slight amounts of this species are consistently observed in the electrochemical and chemical reductions of **3**-M-*p*Cl-MeCN. Because $[Fe_4S_4(SpCl)_4]^{2-}$ is not present in solutions of **3**-M-*p*Cl-MeCN, $[Fe_4S_4(SpCl)_4]^{3-}$ arises from slight degradation of **5**-M-*p*Cl-MeCN. The reduced clusters, solvated and ligated (vide infra), exhibit isotropically shifted resonances (Table IV), showing that they are paramagnetic. Isotropic shifts are larger than those of analogous oxidized clusters, indicating that $S > {}^3/_2$ if the shifts are dominantly contact in origin. The latter point is qualitatively supported by the alternating signs of *o*-, *m*-, and *p*-H isotropic shifts[23] of oxidized[5] and reduced clusters. The *m*-H chemical shift of −16.4 ppm for **5**-Mo-*p*Cl-MeCN is very close to that of $[Mo_2Fe_6S_8(SPh)_9]^{5-}$ (−16.1 ppm), for which magnetic susceptibility results indicate the presence of two $S = 2$ subclusters.[3] This spin state is probable for solvated and ligated reduced clusters.

(c) Ligated Clusters. In contrast to quantitative formation of **4**-M-*p*Cl-S*p*Cl in reaction 4 with 1.0 equiv of thiolate, a 20-fold

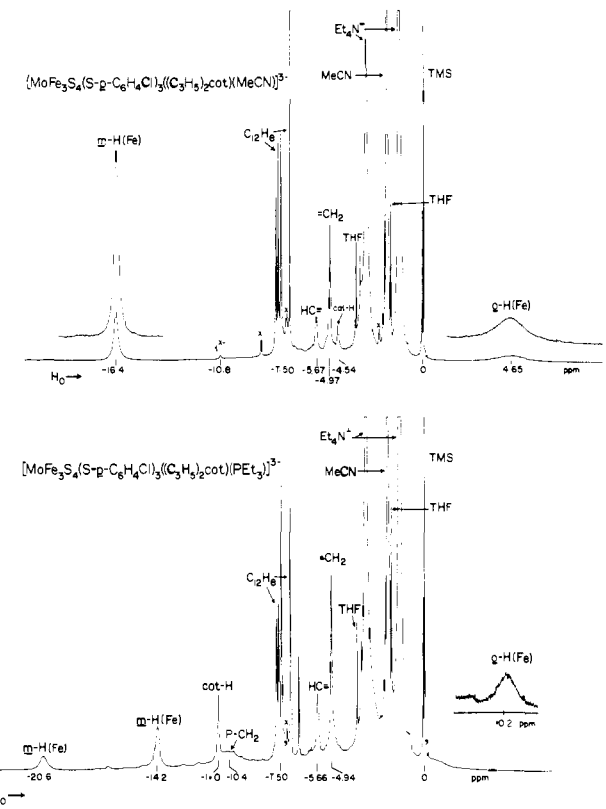

Figure 8. ^{1}H NMR spectra (300 MHz, ~297 K) of ~7 mM solutions of **5**-Mo-*p*Cl-MeCN and **6**-Mo-*p*Cl-PEt_3 in CD_3CN. The reduced cluster was generated by reaction with 1.0 equiv of sodium acenaphthylenide in THF-d_8 and converted to the ligated cluster by reaction with 1.0 equiv of PEt_3. Signal assignments are indicated ($t^{3-} = [Fe_4S_4(SpCl)_4]^{3-}$, $C_{12}H_8$ = acenaphthylene, x = impurity).

excess of this ligand caused no change in the NMR spectrum of ~10 mM **5**-Mo-*p*Cl-MeCN. Thus the reduced cluster has a markedly diminished affinity for this anionic ligand. Reaction of **5**-M-*p*Cl-MeCN with 1.0 equiv of PEt_3 results in essentially quantitative formation of **6**-M-*p*Cl-PEt_3. The spectrum of the M = Mo adduct is provided in Figure 8. Both clusters show two *m*-H signals whose weighted mean shifts are within 0.1–0.2 ppm of the shifts of the precursor solvated clusters. Hence these species, as their oxidized counterparts **4**-M-R-L, have structures of effective C_s symmetry. An additional conspicuous feature of the spectra of the phosphine adducts is the occurrence of cat-H resonances at −11.0 (Mo) and −9.28 (W) ppm, representing downfield displacements of ca. 5–6 ppm as a consequence of phosphine binding. The spectrum of **6**-Mo-*p*Cl-PEt_3 was unaffected by the presence of a 5-fold excess of PEt_3, indicating the absence of further ligation with the cluster and (with this excess) of a ligand exchange process.

Exposure of a ~6 mM solution of **5**-Mo-*p*Cl-MeCN to 1–2 equiv of CO in Ar produced a species with an intense carbonyl band at 1810 cm^{-1}. The infrared spectrum, which did not change appreciably over a 160-min period, is shown in Figure 9. Absorption spectra showed that no appreciable cluster oxidation had occurred in the process. Removal of all volatiles in vacuo and dissolution of the residue in acetonitrile afforded a solution whose spectrum retained the 1810-cm^{-1} band. This observation indicates the CO binding is not reversible. The cluster **5**-W-*p*Cl-MeCN proved to be more reactive to CO under comparable conditions. The spectrum resulting from exposure to 0.5 equiv of CO in Ar for 15 min (Figure 8) contains an intense band at 1790 cm^{-1} and two much weaker features. Larger amounts of CO and longer reaction times resulted in the disappearance of the initial strong bands in both the M = Mo and W systems and the appearance of multiple band spectra containing features in the range 1840–1980 cm^{-1}. This situation with the latter system is illustrated in Figure 9. None of the species responsible for these more

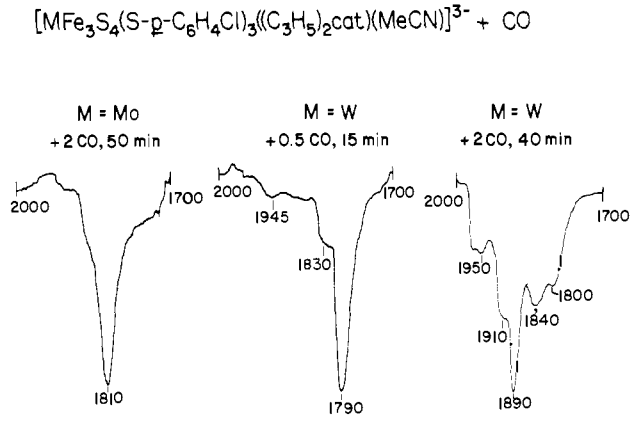

Figure 9. Infrared spectra (l = 0.5 mm) of the reaction products of **5**-M-*p*Cl-MeCN in acetonitrile solutions: left, 7.1 mM **5**-Mo-*p*Cl-MeCN + 2.0 equiv of CO/Mo after 50 min; center, 6.7 mM **5**-W-*p*Cl-MeCN + 0.5 equiv of CO/W after 15 min; right, 6.7 mM **5**-W-*p*Cl-MeCN + 2 equiv of CO/W after 40 min. Frequencies are in cm^{-1}.

complicated spectra have been identified. Because 1810- and 1790-cm^{-1} species are the first to appear in the presence of small amounts of CO, they are tentatively ascribed to the clusters **6**-M-*p*Cl-CO. The solvated oxidized clusters, when exposed to ≥20 equiv of CO for at least 70 min, showed no reaction by infrared spectral examination. Lastly, reaction systems containing **5**-M-*p*Cl-MeCN and ≥1 equiv of $(Et_4N)CN$ or $PhCH_2NC$ have been briefly examined. Multiple resonances in the −10 to −20 ppm range were observed, indicating the formation of more than one new species, none of which could be clearly identified as **6**-M-*p*Cl-L by NMR criteria.

Summary

The following are the principal results and conclusions of this investigation.

(i) Reaction of the oxidized solvate clusters, **3**-M-R-MeCN (M = Mo, W), formed in solution from the doubly-bridged double cubanes **2**-M, with 1.0 equiv of the ligands L = S*p*Cl$^-$, CN$^-$, OPh$^-$, and PEt_3 results in quantitative formation of the ligated clusters **4**-M-R-L, examples of all of which except the (very soluble) phosphine species have been isolated in 54–77% purified yields as Et_4N^+ salts. Carbon monoxide does not react with oxidized solvate clusters.

(ii) The crystal structure of $(Et_4N)_2[MoFe_3S_4(S\text{-}p\text{-}C_6H_4Cl)_4(C_3H_5)_2cat)]$ contains the individual cluster **4**-Mo-*p*Cl-S*p*Cl of C_s near-symmetry, and provides the first unequivocal demonstration of a MFe_3S_4 single cubane.[4] The Mo–S*p*Cl bond length of 2.600 (3) Å is emphatically longer than other terminal Mo(II–IV)–SR distances (range 2.24–2.37 Å[27,28]), and it and the terminal Fe–SR distances are 0.04–0.09 Å shorter than bridge Mo–SR and Fe–SR distances in **2**-M. Bridge bond lengthening provides a plausible rationale of the ready cleavage of the double cubanes **2**-M in coordinating solvents.

(iii) All clusters **3**-M-R-solv and **4**-M-R-L exhibit chemically reversible reductions and some sustain similarly reversible oxidations, affording the electron-transfer series (eq 6). The reduced solvated clusters **5**-M-*p*Cl-MeCN may be generated in solution by reaction of **3**-M-*p*Cl-MeCN with sodium acenaphthylenide, causing characteristic spectral changes (Figure 6) and elimination of the $S = {}^3/_2$ type EPR spectra of the oxidized clusters.

(iv) The clusters **5**-M-*p*Cl-MeCN do not react with a 20-fold excess of S*p*Cl$^-$, indicating decreased affinity of reduced vs. oxidized clusters for anionic ligands, and quantitatively form **6**-M-*p*Cl-PEt_3 with 1.0 equiv of PEt_3.

(v) All ligated oxidized and reduced clusters in (i) and (iv) have structures of effective C_s symmetry in acetonitrile solutions, on the basis of the existence of two resonances (1:2 intensity ratio) of Fe-bound ligands.

(vi) If formation of the initial reaction products between **5**-M-*p*Cl-MeCN and CO as **6**-M-*p*Cl-CO (ν_{CO} = 1810 (Mo), 1790 (W) cm^{-1}) is accepted, comparison of ν_{CO} (Mo) with those of other Mo *mono*carbonyl complexes indicates that $[MoFe_3S_4(S\text{-}p\text{-}C_6H_4Cl)_3((C_3H_5)_2cat)]^{3-}$ is a π donor comparable with $(C_5H_5)Mo(PBu_3)_2I$ (1804 cm^{-1}),[29] $Mo(S_2CNEt_2)(dpe)$ (1790 cm^{-1}),[30] $Mo(dpe)_2$ (1807 cm^{-1}),[31] and $Mo(N_2)(dpe)_2$ (1799 cm^{-1}).[31]

With means of formation and spectroscopic characterization of reduced solvated clusters now available, the reactivity properties of these species toward reducible substrates are under study. The presence of substitutionally labile solvate ligands provides the opportunity, considered earlier,[1,5] for substrate binding and activation at the Mo atom site. Systems of prime interest are those composed of reduced clusters, carriers capable of electron transfer to oxidized clusters (formed in substrate reactions), protic molecules (for H_2 evolution), and acetylene and dinitrogen in the presence of protic sources. On the basis of EXAFS criteria[6,7] cubane-type $MoFe_3S_4$ clusters continue as viable synthetic representations of the Mo atom coordination site in nitrogenase and FeMo-co.

Acknowledgment. This research was supported by NSF Grant CHE 81-06017. X-ray and NMR equipment used in this research was obtained by NSF Grants CHE 80-00670 and CHE 80-08891.

Registry No. 2-W-pCl, 84143-03-3; **2**-W-Et, 82247-33-4; **2**-Mo-pCl, 82247-34-5; **3**-Mo-pCl-MeCN, 80702-98-3; **3**-Mo-Et-Me_2SO, 84130-66-5; **3**-W-pCl-MeCN, 84130-67-6; **3**-W-Et-Me_2SO, 84130-68-7; **3**-Mo-pCl-DMF, 84130-70-1; **3**-W-pCl-DMF, 84130-71-2; **3**-Mo-pCl-Me_2SO, 84130-72-3; **3**-W-pCl-Me_2SO, 84130-73-4; **4**-Mo-pCl-SpCl, 80789-40-8; **4**-W-pCl-SpCl, 84130-54-1; **4**-Mo-pCl-CN, 80764-35-8; **4**-W-pCl-CN, 84130-56-3; **4**-Mo-Et-CN, 84130-58-5; **4**-W-Et-CN, 84130-60-9; **4**-Mo-pCl-OPh, 80764-37-0; **4**-Mo-pCl-PEt_3, 84130-69-8; (**4**-Mo-pCl)$_2$dmpe, 84143-05-5; **5**-Mo-pCl-MeCN, 84143-04-4; **5**-W-pCl-MeCN, 84130-61-0; **6**-W-pCl-PEt_3, 84130-63-2; **6**-Mo-pCl-CO, 84130-64-3; **6**-W-pCl-CO, 84130-65-4; $(Et_4N)(S\text{-}p\text{-}C_6H_4Cl)$, 84143-01-1; $(Et_4N)(OPh)$, 32580-85-1; *p*-chlorobenzenethiol, 106-54-7; phenol, 108-95-2; **2**-Mo-Et, 82281-65-0; **6**-Mo-pCl-PEt_3, 84130-62-1.

Supplementary Material Available: Crystal structure data for $(Et_4N)_3[MoFe_3S_4(S\text{-}p\text{-}C_6H_4Cl)_4((C_3H_5)_2cat)]$: thermal parameters of cations and anion (Table S-I); positional parameters of cations (Table S-II); unweighted least-squares planes of the anion (Table S-III); values of $10|F_o|$ and $10|F_c|$ (Table S-IV) (38 pages). Ordering information is given on any current masthead page.

(27) Chisholm, M. H.; Corning, J. F.; Huffman, J. C.; *Inorg. Chem.* **1982**, *21*, 286. Kamata, M.; Hirotsu, K.; Higuchi, T.; Tatsumi, K.; Hoffmann, R.; Yoshida, T.; Otsuka, S. *J. Am. Chem. Soc.* **1981**, *103*, 5772. Kamata, M.; Yoshida, T.; Otsuka, S.; Hirotsu, K.; Higuchi, T. *Ibid.* **1981**, *103*, 3572. Otsuka, S.; Kamata, M.; Hirotsu, K.; Higuchi, T. *Ibid.* **1981**, *103*, 3012. Condon, D.; Ferguson, G.; Lalor, F. J.; Parvez, M.; Spalding, T. *Inorg. Chem.* **1982**, *21*, 188. Begley, T.; Condon, D.; Ferguson, G.; Lalor, F. J.; Khan, M. A. *Ibid.* **1981**, *20*, 3420. Hyde, J.; Magin, L.; Zubieta, J. *J. Chem. Soc., Chem. Commun.* **1980**, 204. Hyde, J.; Zubieta, J.; Seeman, N. *Inorg. Chim. Acta* **1981**, *54*, L137.

(28) Analysis of charge distribution in $[Mo_2Fe_6S_8(SPh)_9]^{3-,4-,5-}$ based on ^{57}Fe isomer shifts suggests that the Mo atom in clusters isoelectronic with **4**-Mo-R-L is reasonably described as Mo(III).[3]

(29) Manning, A. R. *J. Chem. Soc. A* **1967**, 1984.

(30) Crichton, B. A. L.; Dilworth, J. R.; Picket, C. J.; Chatt, J. *J. Chem. Soc., Dalton Trans.* **1982**, 892 (dpe = $Ph_2PCH_2CH_2PPh_2$).

(31) Sato, M.; Tatsumi, T.; Kodama, T.; Hidai, M.; Uchida, T.; Uchida, Y. *J. Am. Chem. Soc.* **1978**, *100*, 4447.